

KEK-CP-278
OU-HET-765-2012
UTHEP-646

Chiral behavior of kaon semileptonic form factors in lattice QCD with exact chiral symmetry

JLQCD Collaboration: T. Kaneko^{*a,b,†}, S. Aoki^{c,d}, G. Cossu^a, X. Feng^a, H. Fukaya^e, S. Hashimoto^{a,b}, J. Noaki^a and T. Onogi^e

^a High Energy Accelerator Research Organization (KEK), Ibaraki 305-0801, Japan

^b School of High Energy Accelerator Science, The Graduate University for Advanced Studies (Sokendai), Ibaraki 305-0801, Japan

^c Graduate School of Pure and Applied Sciences, University of Tsukuba, Ibaraki 305-8571, Japan

^d Center for Computational Sciences, University of Tsukuba, Tsukuba, Ibaraki 305-8577, Japan

^e Department of Physics, Osaka University, Toyonaka, Osaka 560-0043, Japan

We calculate the kaon semileptonic form factors in lattice QCD with three flavors of dynamical overlap quarks. Gauge ensembles are generated at pion masses as low as 290 MeV and at a strange quark mass near its physical value. We precisely calculate relevant meson correlators using the all-to-all quark propagator. Twisted boundary conditions and the reweighting technique are employed to vary the momentum transfer and the strange quark mass. We discuss the chiral behavior of the form factors by comparing with chiral perturbation theory and experiments.

*The 30 International Symposium on Lattice Field Theory - Lattice 2012,
June 24-29, 2012
Cairns, Australia*

^{*}Speaker.

[†]E-mail: takashi.kaneko@kek.jp

1. Introduction

Precise determination of the Cabibbo-Kobayashi-Maskawa (CKM) matrix elements provides a stringent test of the Standard Model to search for new physics. One of the elements $|V_{us}|$ can be determined from the $K \rightarrow \pi l \nu$ decays through a theoretical calculation of the normalization of the vector form factor $f_+(0)$, which parametrizes the $K \rightarrow \pi$ matrix element

$$\langle \pi(p') | V_\mu | K(p) \rangle = (p + p')_\mu f_+(q^2) + (p - p')_\mu f_-(q^2) \quad (q^2 = (p - p')^2). \quad (1.1)$$

In this article, we report on our calculation of $f_+(0)$ in $N_f = 2+1$ lattice QCD within 1 % accuracy. In order to demonstrate the reliability of this precise calculation, we also examine the consistency of other quantities, such as $f_-(0)$ and the form factors' shape, with chiral perturbation theory (ChPT) and experiments.

2. Calculation of form factors

We employ the overlap quark action to exactly preserve chiral symmetry for a straightforward comparison of $f_{\{+,-\}}(q^2)$ with ChPT. Numerical simulations are accelerated by modifying the Iwasaki gauge action [1] and by simulating the trivial topological sector [1, 2]. Effects of the fixed topology are suppressed by the inverse of the lattice volume $N_s^3 \times N_t$ [2]. We use our gauge ensembles generated at a single lattice spacing $a = 0.112(1)$ fm, which is determined from the Ω baryon mass, and at a strange quark mass $m_s = 0.080$, which is close to its physical value $m_{s,\text{phys}} = 0.081$. We simulate four values of degenerate up and down quark masses $m_{ud} = 0.015, 0.025, 0.035$ and 0.050 that cover a range of the pion mass 290–540 MeV. At each m_{ud} , a lattice size of $16^3 \times 48$ or $24^3 \times 48$ is chosen to control finite volume effects by satisfying a condition $M_\pi L \gtrsim 4$. The statistics are 2,500 HMC trajectories at each combination of m_{ud} and m_s .

We calculate the scalar form factor $f_0(q^2) = f_+(q^2) + f_-(q^2) q^2 / (M_K^2 - M_\pi^2)$ at $q^2 = q_{\text{max}}^2 = (M_K - M_\pi)^2$, $f_+(q^2)$ and $\xi(q^2) = f_-(q^2) / f_+(q^2)$ at $q^2 < q_{\text{max}}^2$ from the following ratios [3]

$$R = \frac{C_4^{K\pi}(\Delta t, \Delta t'; \mathbf{0}, \mathbf{0}) C_4^{\pi K}(\Delta t, \Delta t'; \mathbf{0}, \mathbf{0})}{C_4^{KK}(\Delta t, \Delta t'; \mathbf{0}, \mathbf{0}) C_4^{\pi\pi}(\Delta t, \Delta t'; \mathbf{0}, \mathbf{0})} \xrightarrow{\Delta t, \Delta t' \rightarrow \infty} \frac{(M_K + M_\pi)^2}{4M_K M_\pi} f_0(q_{\text{max}}^2)^2, \quad (2.1)$$

$$\tilde{R} = \frac{C_4^{K\pi}(\Delta t, \Delta t'; \mathbf{p}, \mathbf{p}') C^K(\Delta t, \mathbf{0}) C^\pi(\Delta t', \mathbf{0})}{C_4^{K\pi}(\Delta t, \Delta t'; \mathbf{0}, \mathbf{0}) C^K(\Delta t, \mathbf{p}) C^\pi(\Delta t', \mathbf{p}')} \rightarrow \left\{ \frac{E_K + E'_\pi}{M_K + M_\pi} + \frac{E_K - E'_\pi}{M_K + M_\pi} \xi(q^2) \right\} \frac{f_+(q^2)}{f_0(q_{\text{max}}^2)}, \quad (2.2)$$

$$R_k = \frac{C_k^{K\pi}(\Delta t, \Delta t'; \mathbf{p}, \mathbf{p}') C_k^{KK}(\Delta t, \Delta t'; \mathbf{p}, \mathbf{p}')}{C_4^{K\pi}(\Delta t, \Delta t'; \mathbf{p}, \mathbf{p}') C_k^{KK}(\Delta t, \Delta t'; \mathbf{p}, \mathbf{p}')} \rightarrow \frac{E_K + E'_K}{(p + p')_k} \frac{(p + p')_k + (p - p')_k \xi(q^2)}{E_K + E'_\pi + (E_K - E'_\pi) \xi(q^2)} \quad (2.3)$$

where $E_p^{(\prime)}$ ($P = \pi$ or K) represents the meson energy with the spatial momentum $\mathbf{p}^{(\prime)}$. Note that these observables are sufficient to determine $f_{\{+,-,0\}}(q^2)$ at simulated values of q^2 , except at q_{max}^2 , where \tilde{R} and R_k have no sensitivity to $\xi(q^2)$. Two- and three-point functions are defined as

$$C^P(\Delta t, \mathbf{p}) = \frac{1}{N_s^3 N_t} \sum_{\mathbf{x}, t} \sum_{\mathbf{x}'} \langle \mathcal{O}_P(\mathbf{x}', t + \Delta t) \mathcal{O}_P^\dagger(\mathbf{x}, t) \rangle e^{-i\mathbf{p}(\mathbf{x}' - \mathbf{x})}, \quad (2.4)$$

$$C_\mu^{PQ}(\Delta t, \Delta t'; \mathbf{p}, \mathbf{p}') = \frac{1}{N_s^3 N_t} \sum_{\mathbf{x}, t} \sum_{\mathbf{x}'', \mathbf{x}'} \langle \mathcal{O}_Q(\mathbf{x}'', t + \Delta t + \Delta t') V_\mu(\mathbf{x}', t + \Delta t) \mathcal{O}_P^\dagger(\mathbf{x}, t) \rangle \\ \times e^{-i\mathbf{p}'(\mathbf{x}'' - \mathbf{x}') - i\mathbf{p}(\mathbf{x}' - \mathbf{x})}, \quad (2.5)$$

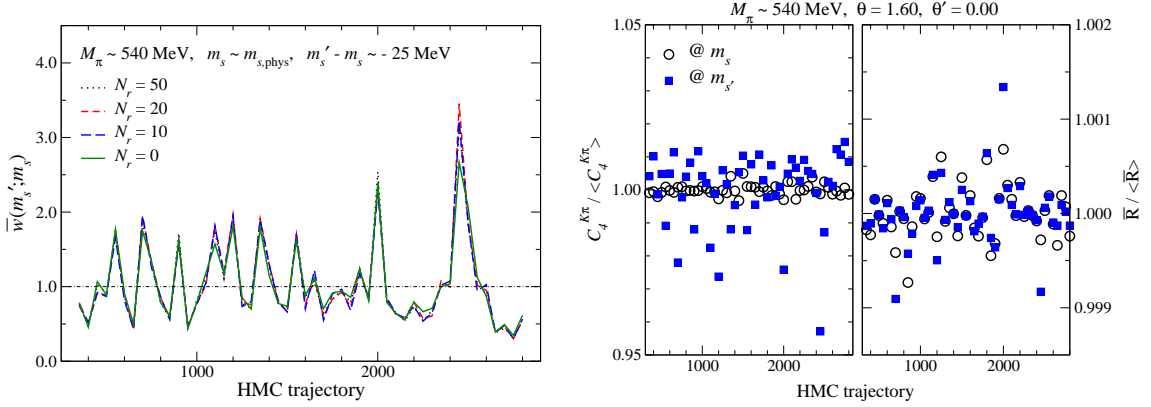


Figure 1: Left panel: Monte Carlo history of normalized reweighting factor $\tilde{w}(m'_s, m_s)$ at our largest m_{ud} . Four lines show data with different numbers of noise samples (N_r). Right panel: statistical fluctuation of $C_4^{K\pi}$ and \tilde{R} before (open symbols) and after (filled symbols) reweighting. $\theta^{(i)}$ represents the twist angle used to induce the initial (final) meson momentum $\mathbf{p}^{(i)}$.

where $\mathcal{O}_{P(Q)}^\dagger(\mathbf{x}, t)$ ($P, Q = \pi$ or K) represents the meson interpolating operator $\sum_{\mathbf{r}} \phi(\mathbf{r}) \bar{q}(\mathbf{x} + \mathbf{r}, t) \gamma_5 q'(\mathbf{x}, t)$ with an exponential smearing function $\phi(\mathbf{r}) = e^{-0.4|\mathbf{r}|}$. We use the all-to-all propagator [4, 5] to remarkably improve the statistical accuracy of the correlators and, hence, form factors [6, 7].

In order to precisely determine $f_+(0)$, we explore the most important kinematical region $q^2 \sim 0$ by using the twisted boundary conditions (TBCs) [8]

$$q(\mathbf{x} + N_s \hat{k}, t) = e^{i\theta} q(\mathbf{x}, t), \quad \bar{q}(\mathbf{x} + N_s \hat{k}, t) = e^{-i\theta} \bar{q}(\mathbf{x}, t) \quad (k = 1, 2, 3), \quad (2.6)$$

where \hat{k} is a unit vector in the k -th direction. For simplicity, we use a common twist angle θ in all three spatial directions and take four (three) values of θ (including $\theta = 0$) to cover $-0.1 \lesssim q^2 [\text{GeV}^2] \leq q_{\text{max}}^2$ on the $16^3 \times 48$ ($24^3 \times 48$) lattice.

3. Reweighting

The strange quark mass dependence of the form factors is studied by simulating a different value $m'_s = 0.060$, which is about 25 MeV smaller than $m_s = 0.080$. We employ the reweighting technique in which an observable \mathcal{O} at m'_s is calculated on the gauge configurations at m_s as

$$\langle \mathcal{O} \rangle_{m'_s} = \langle \mathcal{O} \tilde{w}(m'_s, m_s) \rangle_{m_s}, \quad \tilde{w}(m'_s, m_s) = \frac{w(m'_s, m_s)}{\langle w(m'_s, m_s) \rangle_{m_s}}, \quad w(m'_s, m_s) = \frac{\det[D(m'_s)]}{\det[D(m_s)]}, \quad (3.1)$$

where $\langle \dots \rangle_{m_s^{(i)}}$ and $D(m_s^{(i)})$ represent the Monte Carlo average and the overlap-Dirac operator at the strange quark mass $m_s^{(i)}$, respectively. We consider decomposing the reweighting factor w into contributions of low- and high-modes of D as $w = w_{\text{low}} w_{\text{high}}$. The low-mode contribution $w_{\text{low}} = \prod_k \lambda_k(m'_s) / \prod_k \lambda_k(m_s)$ is exactly calculated by using 160 (240) low-lying eigenvalues λ_k on $16^3 \times 48$ ($24^3 \times 48$). A noisy estimator is employed for $w_{\text{high}}^2 = (1/N_r) \sum_{r=1}^{N_r} \exp[-(\bar{P} \xi_r)^\dagger (\Omega - 1) (\bar{P} \xi_r) / 2]$ with $\Omega = D(m_s)^\dagger \{D(m'_s)^{-1}\}^\dagger D(m'_s)^{-1} D(m_s)$, where $\{\xi_1, \dots, \xi_{N_r}\}$ is a set of Gaussian noise vectors, and \bar{P} projects them to the eigenspace spanned by the high-modes.

The left panel of Fig. 1 shows the Monte Carlo history of the normalized reweighting factor \tilde{w} , which appears in the expression of the observable in Eq. (3.1). With our simulation setup, \tilde{w} has small dependence on the number of the noise vectors N_r . From this observation, we set $N_r = 10$ to precisely calculate \tilde{w} on each gauge configuration.

The right panel of Fig. 1 shows how reweighting affects the statistical accuracy of the correlator $C_4^{K\pi}$ and the ratio \tilde{R} . The fluctuation of $C_4^{K\pi}$ is largely enhanced by \tilde{w} , which is typically in the range of $[0.5, 2.0]$. We observe, however, that the enhanced fluctuations are largely canceled in the ratio \tilde{R} . Consequently, the statistical accuracies of the form factors are not largely impaired by reweighting: typically $\lesssim 1.0\%$ (20%) for $f_{\{+,0\}}(q^2)$ ($\xi(q^2)$) before reweighting, and $\lesssim 1.5\%$ (30%) after reweighting.

4. q^2 dependence of form factors

Our results for $f_0(q^2)$ at the smallest m_{ud} are plotted as a function of q^2 in the left panel of Fig. 2. We use TBCs to simulate small values of $|q^2|$, where contributions of higher orders in q^2 are small and our data are well described by any of the following parametrization forms

$$f_0(q^2) = f_0(0)(1 + c_1 q^2), \quad f_0(q^2) = f_0(0)(1 + c_1 q^2 + c_2 q^4), \quad f_0(q^2) = \frac{f_0(0)}{1 - q^2/M_{\text{pole}}^2}. \quad (4.1)$$

A different form $f_+(0) \{1/(1 - q^2/M_{K^*}^2) + c_1 q^2\}$ with the K^* pole plus a polynomial correction is also tested for $f_+(q^2)$. We confirm a good agreement among $f_+(0)$ and $f_0(0)$ obtained from these parametrizations as shown in the right panel of Fig. 2. In this report, we employ a simultaneous fit using the quadratic form for f_0 and the form with the K^* pole for f_+ to determine the normalization $f_+(0)$ and its slope $f'_+(0)$. The uncertainty of this interpolation is estimated by using the different parametrization forms and turns out to be similar to or smaller than the statistical error.

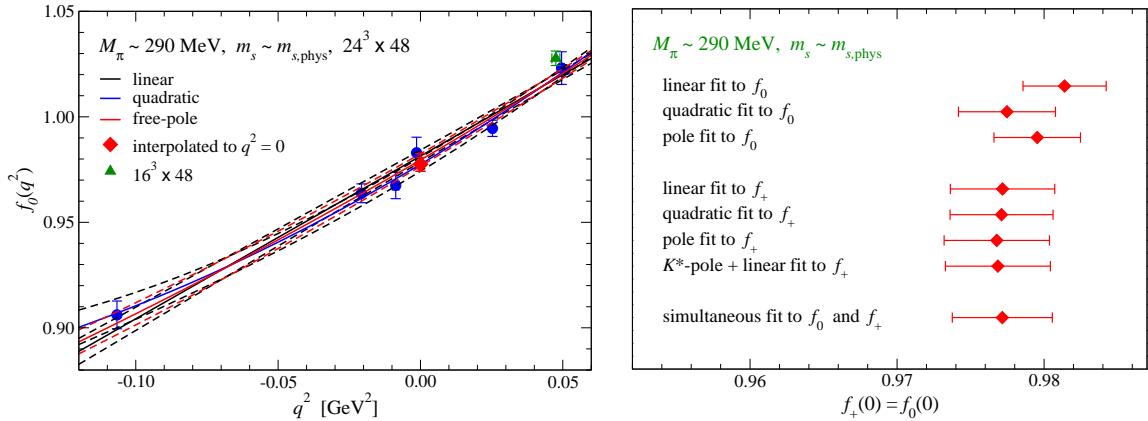


Figure 2: Left panel: scalar form factor $f_0(q^2)$ at our smallest m_{ud} as a function of q^2 . We plot interpolations listed in Eq. (4.1) together with $f_0(0)$ determined from the quadratic parametrization (diamond). Our result on a smaller lattice $16^3 \times 48$ is also plotted to examine finite volume effects (triangle). Right panel: comparison of $f_+(0)$ ($= f_0(0)$) obtained by using different parametrization forms.

In the left panel of Fig. 2, we also plot a result of $f_0(q^2)$ obtained on a smaller lattice $16^3 \times 48$. The difference from $24^3 \times 48$ can be attributed to the conventional finite volume effect as well as the fixed topology effect, but turns out to be insignificant (0.8 %, 2.1 σ). The finite volume effect remaining on the larger volume $24^3 \times 48$ is estimated as $\lesssim 0.3$ % by assuming the $1/N_s^3 N_t$ scaling of the fixed topology effect and can be safely neglected in the following analysis.

5. Chiral extrapolation of $f_+(0)$

There are two popular choices of the expansion parameter in ChPT: $\xi_P = M_P^2/(4\pi F_\pi)^2$ and $M_P^2/(4\pi F_0)^2$ ($P = \pi, K, \eta$), where F_0 is the decay constant in the $SU(3)$ chiral limit. The latter choice largely enhances the chiral corrections in $f_+(0)$ [7] and leads to worse convergences in the expansions of M_P and f_P [9]. We therefore use the former and denote the chiral expansion as $f_+(0) = 1 + f_2 + \Delta f$, where f_2 and Δf are $O(\xi_P)$ and higher order contributions, respectively.

The Ademollo-Gatto theorem $f_+(0) - 1 \propto (m_s - m_{ud})^2$ [10] guarantees that f_2 [11]

$$f_2 = \frac{3}{2} (H_{K\pi} + H_{K\eta}), \quad H_{PQ} = -\frac{\xi_P + \xi_Q}{8} \left(1 + \frac{2\xi_P \xi_Q}{\xi_P^2 - \xi_Q^2} \ln \left[\frac{\xi_Q}{\xi_P} \right] \right) \quad (5.1)$$

is written in terms of physical observables $\xi_{\{\pi, K, \eta\}}$ and does not contain low-energy constants (LECs) in the ChPT Lagrangian. The chiral expansion of $f_+(0)$ is then nothing but the parametrization of Δf . In the left panel of Fig. 3, we examine the quark mass dependence of Δf divided by $(M_K^2 - M_\pi^2)^2$ which is motivated by the Ademollo-Gatto theorem. The mild dependence suggests that our data can be described by a simple constant fit $\Delta f/(M_K^2 - M_\pi^2)^2 = c_4$ which gives rise to the $O(\xi_P^2)$ analytic term in $f_+(0)$. We also confirm that the chiral extrapolation of $\Delta f/(M_K^2 - M_\pi^2)^2$ is not largely modified by including the following $O(\xi_P^2)$ logarithmic and $O(\xi_P^3)$ analytic corrections

$$\Delta f/(M_K^2 - M_\pi^2)^2 - c_4 = c'_{4,\pi} \log[\xi_\pi], \quad \text{or } c''_{4,\pi} \log^2[\xi_\pi], \quad \text{or } c_{6,\pi} \xi_\pi, \quad \text{or } c_{6,\pi} \xi_\pi + c_{6,K} \xi_K. \quad (5.2)$$

In this report, we employ a parametrization $\Delta f/(M_K^2 - M_\pi^2)^2 = c_4 + c_{6,\pi} \xi_\pi$, all parameters of which are determined reasonably well with an acceptable value of $\chi^2/\text{d.o.f.} \sim 1.6$. The systematic

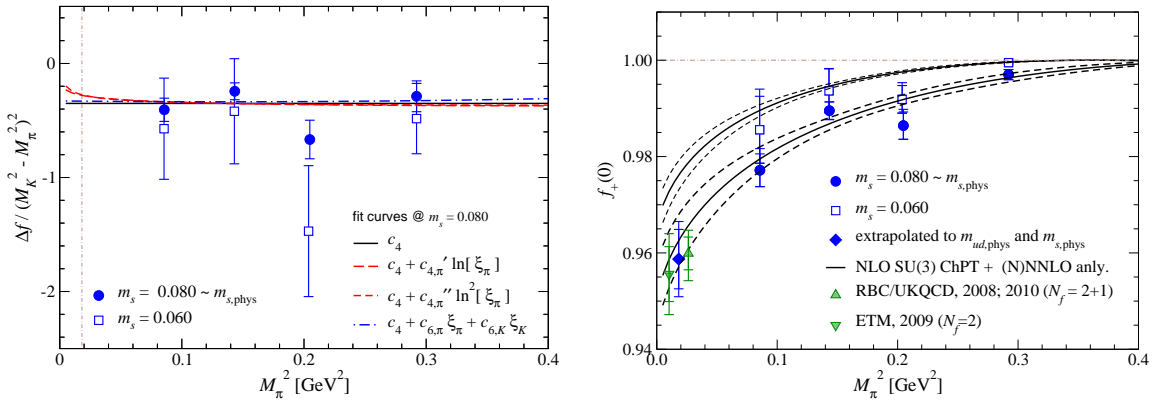


Figure 3: Chiral extrapolations of $\Delta f/(M_K^2 - M_\pi^2)^2$ (left panel) and $f_+(0)$ (right panel). Circles and squares show data at different values of m_s . In the right panel, we also plot $f_+(0)$ from recent calculations in $N_f = 2 + 1$ [12] and $N_f = 2$ [13] QCD.

uncertainty of this extrapolation is estimated as the largest deviation in $f_+(0)$ among the different parametrization forms discussed above. The discretization error in the $SU(3)$ breaking effect $f_2 + \Delta f$ is estimated by an order counting $O((a\Lambda_{\text{QCD}})^2)$ with $\Lambda_{\text{QCD}} \approx 500$. We then obtain

$$f_+(0) = 0.959(6)_{\text{stat}}(4)_{\text{chiral}}(3)_{a \neq 0}, \quad |V_{us}| = 0.2256(19)_{\text{theory+exp't}}, \quad (5.3)$$

where we use $|V_{us}f_+(0)| = 0.2163(5)$ determined from the $K \rightarrow \pi l \nu$ decay rates [14]. Note that previous calculations in $N_f = 2 + 1$ [12] and $N_f = 2$ [13] QCD are consistent with our result.

6. Comparison of $\langle r^2 \rangle_V^{K\pi}$ and $\xi(0)$ with ChPT and experiments

In order to demonstrate the reliability of the 1 % calculation of $f_+(0)$, we compare our data of the normalized slope $\langle r^2 \rangle_V^{K\pi} = 6f'_+(0)/f_+(0)$ and $\xi(0)$ with ChPT and experiments. In contrast to $f_+(0)$, the Ademollo-Gatto theorem is not applicable to these quantities, and unknown LECs appear already in their leading chiral corrections. For $\langle r^2 \rangle_V^{K\pi}$, we parametrize its higher order contributions by simple analytic terms to avoid unstable chiral extrapolations

$$\langle r^2 \rangle_V^{K\pi} = 12L_9^r/F_\pi^2 + \text{“chiral logarithms”} + d_\pi \xi_\pi + d_K \xi_K. \quad (6.1)$$

We refer to Ref. [11] for the explicit expression of the chiral logarithmic terms. The left panel of Fig. 4 shows that this form describes our data reasonably well. It also suggests that the chiral behavior of $\langle r^2 \rangle_V^{K\pi}$ is significantly modified in our simulation region $290 \lesssim M_\pi [\text{MeV}] \lesssim 540$ by the $O(\xi_P)$ contribution at two-loop order in ChPT. We note that significant two-loop corrections have been also observed in our studies of the pion and kaon charge radii [5, 6]. We confirm a good agreement of the extrapolated value of $\langle r^2 \rangle_V^{K\pi}$ with experiment [15]. Our fit result $L_9^r \times 10^3 = 4.3(0.6)_{\text{stat}}(0.3)_{\text{sys}}$ is also consistent with the phenomenological estimate $5.9(0.4)$ [16].

In this report, we parametrize the quark mass dependence of $\xi(0)$ by a simple linear form $\xi(0) = d_0 + d_1(M_K^2 - M_\pi^2)$, which is motivated from the ChPT expression of the leading analytic terms $\propto M_K^2 - M_\pi^2$ [11]. This form describes our data reasonably well as seen in the right panel of Fig. 4. We obtain $d_0 = -0.022(25)$ confirming that $\xi(0)$ vanishes in the $SU(3)$ symmetric limit, as

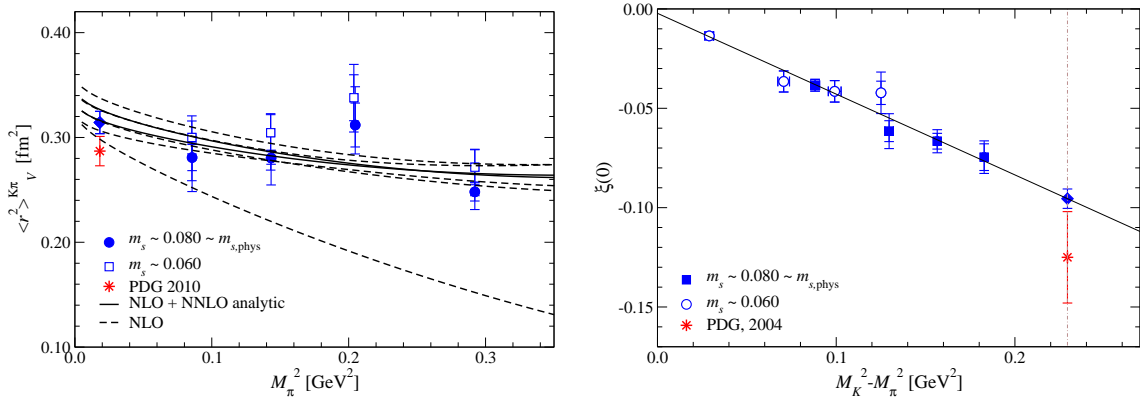


Figure 4: Chiral extrapolation of $\langle r^2 \rangle_V^{K\pi}$ (left panel) and $\xi(0)$ (right panel). In both panels, the diamonds represent our result extrapolated to the physical quark masses m_{ud} and m_s , which should be compared to the experimental values plotted by the stars.

expected. The extrapolation to the physical point yields $\xi(0) = -0.095(5)$ which is consistent with the experimental value $-0.125(23)$ [17].

7. Summary

In this article, we report on our calculation of the kaon semileptonic form factors. The normalization $f_+(0)$ is calculated within 1 % accuracy by utilizing the all-to-all quark propagator, reweighting and TBCs. The reliability of this precise calculation is checked by confirming a good consistency of $\langle r^2 \rangle_V^{K\pi}$ and $\xi(0)$ with experimental results.

Since we observe significant two-loop contributions in the chiral expansions of $f_+(0)$ and $\langle r^2 \rangle_V^{K\pi}$, it is interesting to apply two-loop ChPT formulae to our data. To this end, our use of the overlap quark action is advantageous, since exact chiral symmetry enables us to use the two-loop formulae in the continuum limit without any additional terms at finite lattice spacings. This provides a theoretically clean comparison between lattice QCD and ChPT at the higher order.

Numerical simulations are performed on Hitachi SR11000 and IBM System Blue Gene Solution at High Energy Accelerator Research Organization (KEK) under a support of its Large Scale Simulation Program (No. 11-05) as well as on Hitachi SR16000 at YITP in Kyoto University. This work is supported in part by the Grants-in-Aid for Scientific Research (No. 21674002, 21684013), the Grant-in-Aid for Scientific Research on Innovative Areas (No. 2004: 20105001, 20105002, 20105003, 20105005, 23105710), and SPIRE (Strategic Program for Innovative Research).

References

- [1] H. Fukaya *et al.* (JLQCD collaboration), Phys. Rev. D **74**, 094505 (2006).
- [2] S. Aoki, H. Fukaya, S. Hashimoto and T. Onogi, Phys. Rev. D **76**, 054508 (2007).
- [3] D. Bećirević *et al.*, Nucl. Phys. B **705**, 339 (2005); N. Tsutsui *et al.* (JLQCD Collaboration), PoS **LAT2005**, 357 (2005); C. Dawson *et al.* (RBC Collaboration) Phys. Rev. D **74**, 114502 (2006).
- [4] G.S. Bali *et al.* (SESAM Collaboration), Phys. Rev. D **71**, 114513 (2005); J. Foley *et al.* (TrinLat Collaboration), Comput. Phys. Commun. **172**, 145 (2005).
- [5] S.Aoki *et al.* (JLQCD and TWQCD Collaborations), Phys. Rev. D **80**, 034508 (2009).
- [6] T. Kaneko *et al.* (JLQCD Collaboration), PoS **Lattice 2010**, 146 (2010).
- [7] T. Kaneko *et al.* (JLQCD Collaboration), PoS **Lattice 2011**, 284 (2011).
- [8] P.F. Bedaque, Phys. Lett. B **593**, 82 (2004).
- [9] J. Noaki *et al.* (JLQCD and TWQCD Collaborations), Phys. Rev. Lett. **101**, 202004 (2008); J. Noaki *et al.* (JLQCD and TWQCD Collaborations), PoS **Lattice 2010**, 117 (2010).
- [10] M. Ademollo and R. Gatto, Phys. Rev. Lett. **13**, 264 (1964).
- [11] J. Gasser and H. Leutwyler, Nucl. Phys. B **250**, 517 (1985).
- [12] P.A. Boyle *et al.* (RBC and UKQCD Collaborations), Phys. Rev. Lett. **100**, 141601 (2008).
- [13] V. Lubicz *et al.* (ETM Collaboration), Phys. Rev. D **80**, 111502 (2009).
- [14] M. Antonelli *et al.* (FlaviaNet Working Group on Kaon Decays), Eur. Phys. J. C **69**, 399 (2010).
- [15] K. Nakamura *et al.* (Particle Data Group), J. Phys. G **37**, 075021 (2010).
- [16] J. Bijnens and P. Talavera, JHEP **03**, 046, (2002).
- [17] S. Eidelman *et al.* (Particle Data Group), Phys. Lett. B **592**, 1 (2004).